

Structure-based drug design: the discovery of novel nonpeptide orally active inhibitors of human renin

J Rahuel, V Rasetti, J Maibaum, H Rüeger, R Göschke, N-C Cohen*, S Stutz, F Cumin, W Fuhrer, JM Wood and MG Grütter†

Background: The aspartic proteinase renin plays an important physiological role in the regulation of blood pressure. It catalyses the first step in the conversion of angiotensinogen to the hormone angiotensin II. In the past, potent peptide inhibitors of renin have been developed, but none of these compounds has made it to the end of clinical trials. Our primary aim was to develop novel nonpeptide inhibitors. Based on the available structural information concerning renin–substrate interactions, we synthesized inhibitors in which the peptide portion was replaced by lipophilic moieties that interact with the large hydrophobic S1/S3-binding pocket in renin.

Results: Crystal structure analysis of renin–inhibitor complexes combined with computational methods were employed in the medicinal-chemistry optimisation process. Structure analysis revealed that the newly designed inhibitors bind as predicted to the S1/S3 pocket. In addition, however, these compounds interact with a hitherto unrecognised large, distinct, sub-pocket of the enzyme that extends from the S3-binding site towards the hydrophobic core of the enzyme. Binding to this S3^{sp} sub-pocket was essential for high binding affinity. This unprecedented binding mode guided the drug-design process in which the mostly hydrophobic interactions within subsite S3^{sp} were optimised.

Conclusions: Our design approach led to compounds with high *in vitro* affinity and specificity for renin, favourable bioavailability and excellent oral efficacy in lowering blood pressure in primates. These renin inhibitors are therefore potential therapeutic agents for the treatment of hypertension and related cardiovascular diseases.

Introduction

The renin–angiotensin system (Figure 1) plays a major role in regulating cardiovascular and renal function and in maintaining the electrolyte balance of the body [1–3]. Imbalance may lead to blood pressure abnormalities such as hypertension, or to congestive heart failure. Extensive clinical studies using inhibitors of the angiotensin converting enzyme (ACE) have shown the importance of the renin–angiotensin system in blood-pressure regulation [4,5] and led to the therapeutic application of ACE inhibitors in the treatment of hypertension and congestive heart failure [5–8]. The metabolic degradation of bradykinin and other members of the kinin family by ACE, however, may be responsible for some of the adverse effects of ACE inhibitors [9]. It is therefore desirable to have drugs that influence the formation or action of angiotensin II at other points in the cascade [10–12]. To interfere more specifically with the renin–angiotensin cascade, antagonists of the angiotensin II receptor were developed and introduced to the market [13]. Due to its high specificity for only one substrate, namely angiotensinogen, renin was also identified as an ideal target for antihypertensive drugs. Potent and selective inhibitors

Addresses: Novartis Pharma AG, Metabolic and Cardiovascular Diseases, CH-4002 Basle, Switzerland and Novartis Pharma AG, Core Technology Area, CH-4002 Basle, Switzerland.

Present addresses: *Synergix Drug Design Ltd, Technology Park Malha, Jerusalem 91487, Israel. †Biochemisches Institut, Universität Zürich, Winterthurer Straße 190, CH-8057 Zürich, Switzerland.

Correspondence: Jürgen Maibaum, Markus G Grütter
E-mail: gruetter@biocfebs.unizh.ch
juergen_klaus.maibaum@pharma.novartis.com

Key words: drug design, hypertension, inhibitor binding, renin, X-ray crystallography

Received: 4 February 2000
Revisions requested: 16 March 2000
Revisions received: 28 April 2000
Accepted: 5 May 2000

Published: 16 June 2000

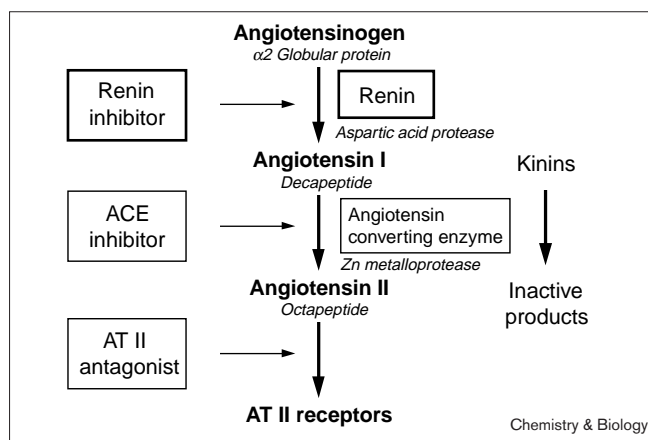
Chemistry & Biology 2000, 7:493–504

1074-5521/00/\$ – see front matter
© 2000 Elsevier Science Ltd. All rights reserved.

of renin could therefore provide a new alternative therapy for the treatment of hypertension without side effects.

Renin (EC 3.4.99.19) is a member of the well-studied family of aspartic proteinases [14,15]. Renin controls the first and rate-limiting step of the renin–angiotensin system catalysing the cleavage of the Leu10–Val11 peptide bond of angiotensinogen and releasing the decapeptide angiotensin I (Figure 1). Angiotensinogen is the only known physiological substrate for renin; therefore renin is an absolutely essential and extremely specific enzyme, in contrast to the angiotensin-converting enzyme (ACE), which can be bypassed by the serine proteinase chymase and is also active against other peptides such as bradykinin. A large variety of peptide inhibitors of human renin with different stable transition-state analogues of the scissile peptide bond have been developed. Because none of these compounds survived all stages of drug development, there was a need for new classes of nonpeptide renin inhibitors that fulfil all criteria for becoming successful drugs. Three-dimensional structures of a number of mammalian and viral aspartic proteinases have been determined. Crystal structures of

Figure 1



The renin-angiotensin cascade. ACE, angiotensin converting enzyme; AT II, angiotensin II.

human and mouse renin in complex with peptide and peptidomimetic inhibitors have been reported (reviewed in [16]; [17–21]). In light of this, we decided to follow a structure-based approach to design novel nonpeptide inhibitors. Here we report the basic concept of our approach, as well as six crystal structures of a selection of the designed inhibitors bound to human renin. The structural information was important for both the validation of the initial design concept and structure-activity optimisation.

Results and discussion

Inhibitor design concept

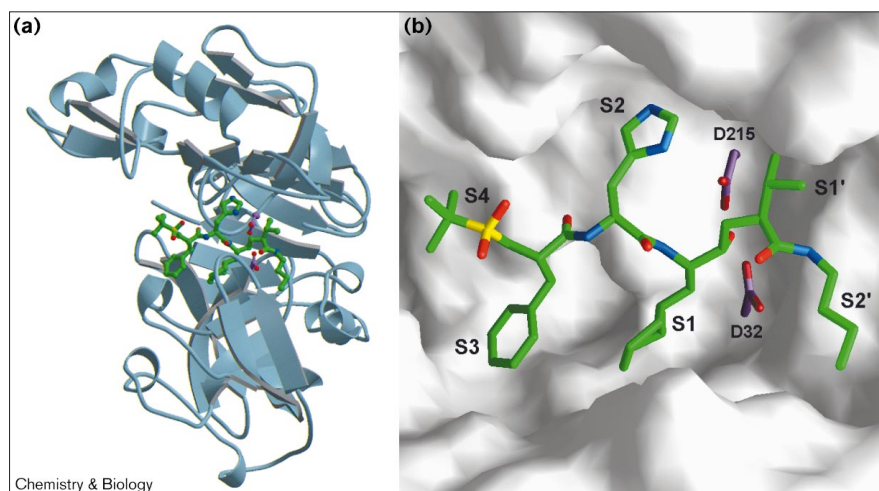
Crystal structures of human renin show that the enzyme consists of two mainly β-sheet domains related by an

approximately twofold axis (Figure 2a). The active-site cleft is located between the two domains and extends over eight residues of the respective substrate. Each domain provides one of the catalytically essential aspartic acid carboxylates (Asp32 and Asp215; residue numbers in this article are according to the pepsin sequence). In all previous peptidic inhibitor-enzyme complexes the inhibitors bind in an extended conformation occupying the active site from the S4 to the S2' subsites (Figure 2).

The initial substrate-based design of inhibitors of renin provided peptide analogues of the amino-terminal part of the substrate angiotensinogen, in which the amino acids flanking the cleavage site were modified [22]. An instrumental approach towards the development of nonsubstrate-based renin inhibitors was the replacement of the scissile Leu10-Val11 dipeptide moiety according to the transition-state analogue concept [23,24], which led to a vast number of *in vitro* highly potent peptide-like (classified recently as type-I inhibitors [25]) renin inhibitors. Poor oral absorption and rapid biliary uptake, resulting from unfavourable lipophilicity and molecular size, are major reasons for the limited bioavailability of most peptide-like renin inhibitors.

The renin inhibitor CGP 38'560 (**1**) [26] as a representative of such type-I inhibitors contains the dipeptide isostere (2*S*,4*S*,5*S*)-5-amino-4-hydroxy-2-isopropyl-6-cyclohexyl-hexanoic acid at the P1-P1' position and mimics the substrate angiotensinogen from residue P3 to P1', according to the Schechter and Berger nomenclature [27]. The compound is a potent and specific inhibitor with an IC₅₀ value of 0.7×10^{-9} M for human renin [28], but it has only a weak blood-pressure lowering effect in salt-depleted marmosets after oral dosing, mainly as a result of very limited overall bioavailability (Table 1).

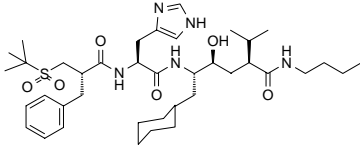
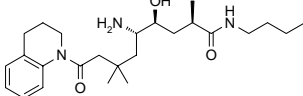
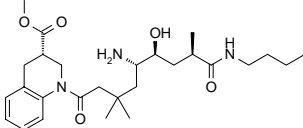
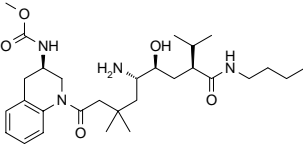
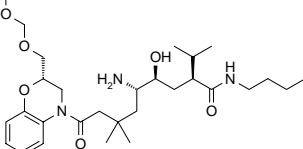
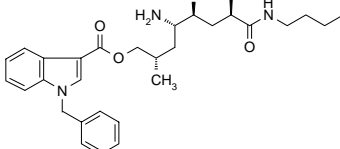
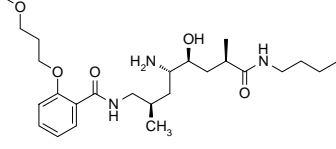
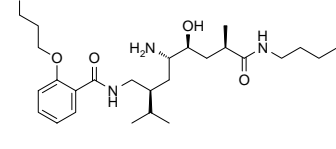
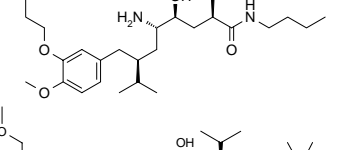
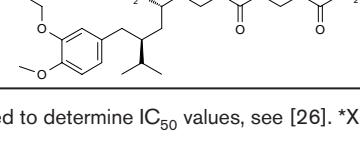
Figure 2



Structure of renin in complex with the peptidic inhibitor CGP 38'560 (**1**). (a) General view of human renin in complex with the inhibitor **1**. Renin is represented as a blue ribbon and the inhibitor as sticks with bonds corresponding to carbon atoms in green. The amino- and carboxy-terminal domains are at the top and at the bottom, respectively (figure made using MOLSCRIPT [49] and Raster3D [50,51]). (b) Closer view of the active site with **1** in the same orientation as in (a). The surface of the enzyme is represented as calculated by the program GRASP [52]. Part of the 'flap' (residues 74–78) as well as residues 110–111, 241–243 and 289 have been removed from the model, previous to calculation of the protein surface, to allow visualization of the active site interior. The inhibitor binds within the active site of renin occupying the binding pockets S4 to S2' in an extended conformation.

Table 1

Biological activity of selected inhibitors of human renin.

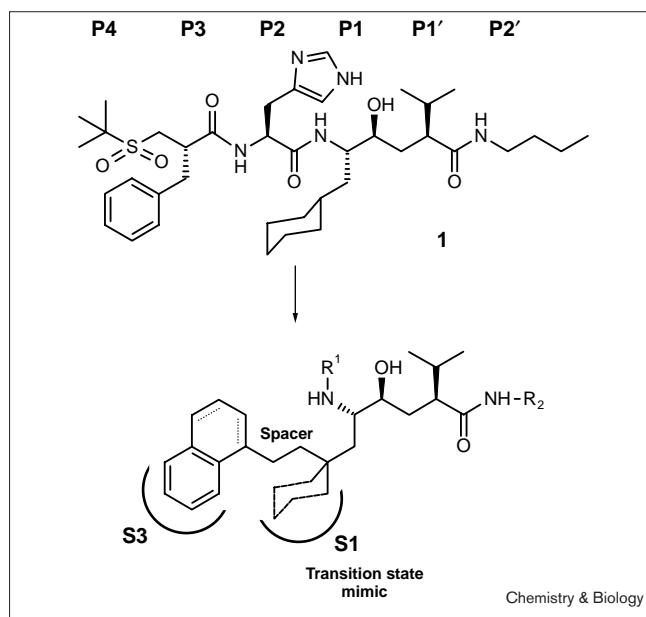
Compound	Formula	IC ₅₀ (μM) Purified human renin	IC ₅₀ (μM) Plasma human renin	IC ₅₀ (μM) Porcine pepsin
1		0.001	0.0007	8.2
2*		0.052	0.043	>100
3		0.0008	0.006	>100
4*		0.0005	0.0004	>100
5*		0.0001	0.0005	>100
6		0.003	0.034	>100
7		0.022	0.026	>100
8		0.0009	0.004	>100
9		0.0004	0.003	>100
10		0.0006	0.0006	>100

For assays used to determine IC₅₀ values, see [26]. *X-ray complex to human renin not determined.

Because of our experience with inhibitor **1** and analogues thereof, the search for nonpeptide inhibitors of lower molecular weight was initiated to identify compounds with good oral bioavailability and efficacy in animal models and stability against metabolic degradation [29,30]. After analysing the shape and chemical properties of the active site of human renin initially using a homology model structure [31], it became apparent that the S1 and S3 pockets form a contiguous and large hydrophobic cavity [30,32]. Applying molecular modelling methods, compounds were designed that would optimally exploit the extended hydrophobic surface corresponding to the large S3–S1 cavity (Figure 2b) and therefore might lead to a sufficient increase in free binding energy through improved van der Waals contacts. At the same time this would allow the elimination of the peptide mainchain from P1 to P4 leading to the nonpeptidic inhibitors as shown in Figure 3. A similar design rationale for human renin inhibitors has also been proposed by two other groups [33,34].

All hydroxyethylene transition-state mimetic inhibitors resulting from this design concept are structurally characterised by a directly linked P1–P3-moiety, and lack the P1–P4 spanning backbone of peptide inhibitors. Variations and extensions of the P3 moiety were explored synthetically and analysed by X-ray crystallography in an iterative design process after the first observation that the ethyl carboxylate group of the P3 heterocycle of inhibitor **3** binds into a deep narrow and well-defined hydrophobic sub-pocket which is accessible from the S3 pocket.

Figure 3



Representation of the P3–P1 structural design approach towards novel nonpeptide renin inhibitors.

Crystal structures of renin complexed with novel nonpeptide inhibitors

The crystal structures of six renin inhibitor complexes have been determined and refined (from this point in the manuscript, 'renin' stands for 'recombinant glycosylated human renin'). Inhibitors with different P3–P1 moieties were chosen (compare with Table 1 for inhibitor structures). In all structures, the electron density for the inhibitor allows them to be positioned in the active site of renin (Figure 4 shows the electron density for inhibitors **6** and **10**). Table 2 summarises the corresponding crystallographic data and refinement statistics. Because structure determinations for the first five inhibitors were performed at room temperature, the observed resolution was between 2.8 and 3.2 Å. The structure of the inhibitor **10**–enzyme complex, carried out at 100 K, was determined at 2.2 Å resolution and is the reference structure for most of the discussion regarding enzyme–inhibitor interactions and differences in enzyme conformation in the two independent molecules of the asymmetric unit of the cubic crystal form.

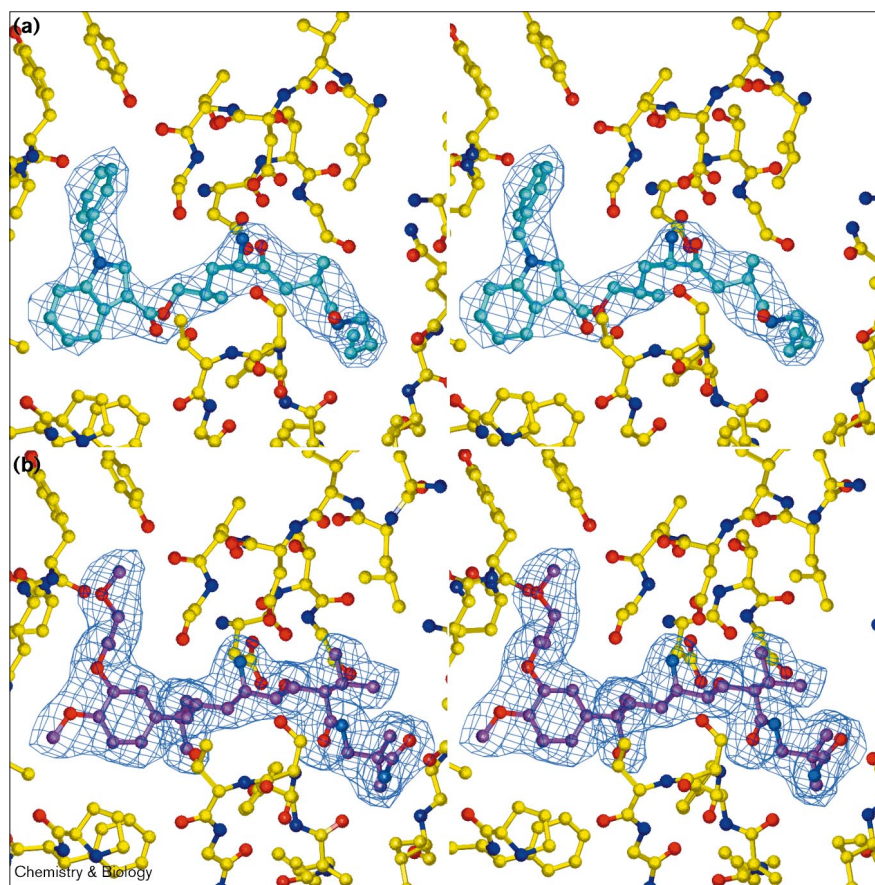
The general fold of renin has already been described in the presence and in the absence of ligand [18]. In short, renin has the predominantly β -sheet fold characteristics of the aspartic protease family. The substrate binding cleft and active site of the enzyme are formed between the two structurally similar amino- and carboxy-terminal domains (Figure 2a). The catalytic residues Asp32 and Asp215 are located in the centre of the cleft. In the cubic crystal form there are two independent renin molecules in the asymmetric unit. One adopts an open and the other a closed conformation. The two conformations differ in the orientation of the carboxy-terminal loops 198–204, 236–254 and 270–286 [18]. These differences do not influence the inhibitor–enzyme interactions directly as illustrated by the comparison of the hydrogen-bond interactions (Table 3). Analysis of the B-factors for the mainchain of the 2.2 Å structure with inhibitor **10** revealed that the closed molecule is more rigid than the open one. The differences reside mainly in the amino-terminal domains as illustrated in the plot of temperature factors (Figure 5).

Binding of small nonpeptide inhibitors

Despite lacking the mainchain P2 to P4, all novel nonpeptide inhibitors are positioned within the extended binding cleft of renin occupying the S3 to S2' subsites. However, an altered hydrogen-bonding pattern as well as binding interactions to a predominantly hydrophobic cavity not utilised by peptide substrates or inhibitors were observed (see below). For comparison a superposition of the inhibitor **10** with the peptide inhibitor CGP 38'560 (**1**) is shown in Figure 6a. Tables 3 and 4 summarise the hydrogen-bond interactions between the inhibitors and renin, and the residues of renin forming the binding pockets occupied by the inhibitors.

Figure 4

Stereoviews of $F_{\text{obs}} - F_{\text{calc}}$ electron-density maps of the active site of renin in the complexes with inhibitors (a) **6** and (b) **10**. The electron densities, calculated after refinement, with the inhibitors omitted, are contoured at 3σ above the mean density. Resolutions are 3.1 and 2.2 Å for complexes containing **6** and **10**, respectively.

**Mainchain hydrogen-bond interactions**

The P2' terminal amide nitrogen of **10** forms a hydrogen bond with the carbonyl oxygen atom of Arg74 (Table 3).

The terminal carbonyl oxygen of the inhibitor is hydrogen bonded to a water molecule, which itself forms a network of hydrogen bonds with the sidechains of Gln128 and

Table 2**Data collection and refinement statistics of complexes of inhibitors with human renin.**

	3	6	7	8	9	10
Space group	P2 ₁ 3	P2 ₁ 3	P4 ₁ 2 ₁ 2	P2 ₁ 3	P2 ₁ 3	P2 ₁ 3
Crystal cell (Å)	a = b = c = 142.9	a = b = c = 143.0	a = b = 98.4 c = 95.6	a = b = c = 142.9	a = b = c = 143.0	a = b = c = 141.6
Resolution (Å)	2.8	3.1	2.9	3.2	3.1	2.2
Observations	59779	57033	38241	43376	59418	187361
Unique	23603	17263	10676	15411	17734	46674
Multiplicity	2.53	3.30	3.58	2.81	3.35	4.01
Completeness (%)	98	96	98	92	99	97
R _{sym}	0.101	0.119	0.062	0.127	0.118	0.065
Program	TNT	XPLOR	XPLOR	XPLOR	TNT	X-PLOR
Resolution range (Å)	10.0–2.8	10.0–3.1	10.0–2.9	10.0–3.2	10.0–3.1	40.0–2.2
Reflections	23086	17263	10398	15335	17183	46674
R factor	0.214	0.217	0.228	0.236	0.210	0.205
						(R _{free} = 0.266)
rms bonds (Å)	0.080	0.019	0.022	0.018	0.082	0.011
rms angles (°)	7.019	3.673	3.730	3.57	7.117	2.03
rms dihedral (°)	28.46	27.33	26.60	27.46	28.56	25.87

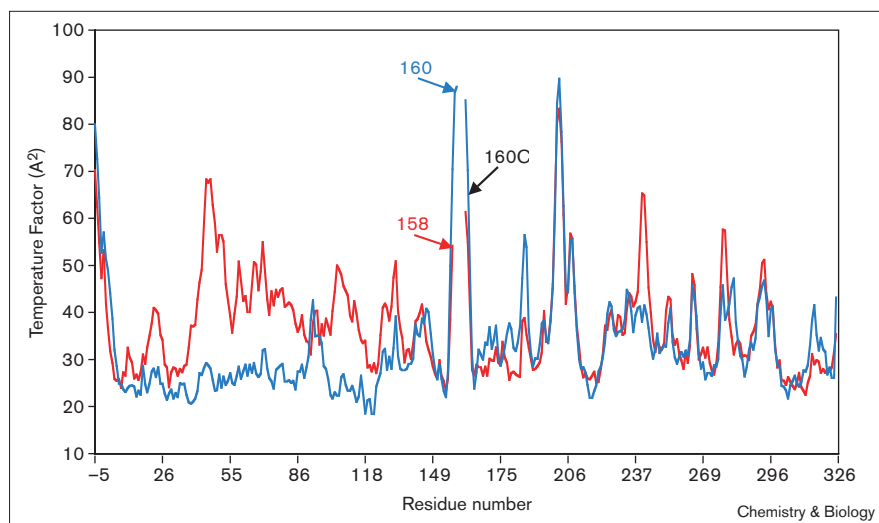
Table 3**Interactions of the inhibitors in the active site of human renin (hydrogen bonds).**

Inhibitor moiety	Inhibitor	Residue and atom of renin	Distance (Å)	
P2' terminal nitrogen	10	Arg74	O	3.0–3.2
P2' nitrogen	all	Gly34	O	2.8–3.9
P1' carbonyl	all	Ser76	N	2.8–3.5
hydroxyl mimic	all	Asp32	O δ 1, O δ 2	2.5–4.1
		Asp215	O δ 1, O δ 2	2.8–4.5
P1 amine	3	Asp32	O δ 1, O δ 2	2.8–4.3
	6	Asp215	O δ 1, O δ 2	2.8–4.1
	7			
	8			
	10			
P1 amine	all	Gly217	O	2.5–4.3
Carbonyl between P3 and P1	3	Thr77	O γ	2.6–3.7
	6			
	7			
	8			
Carbonyl of the P3 substituent	3	Ser219	N	3.2–3.9
		Ser219	O γ	2.8–3.1
Distal ether of the P3 substituent	7	Tyr14	N	2.8–3.1
	8			
	9			
	10			

Minimal and maximal interatomic distances observed between atoms of hydrophilic moieties of the inhibitors and their potential partner in renin. Ranges of interatomic distances listed take into account the distances observed for different inhibitors but also the two forms ('open' and 'closed') observed for complexes studied in the cubic space group (with the exception of inhibitor **7**).

Thr295 residues and with another water molecule. The carboxamide group between P1' and P2' forms hydrogen bonds analogous to substrate or peptide inhibitors (Table 3, Figure 7). In complexes with peptide inhibitors the hydroxyl group of the transition state dipeptide isostere forms hydrogen bonds with both catalytic aspartic

acid residues Asp215 and Asp32 in an almost symmetric manner. In the structures with the nonpeptide inhibitors, the primary amino group substituting the P2–P1 amide group of peptide inhibitors forms hydrogen bonds with the mainchain carbonyl of Gly217 and the carboxylate of Asp215 and in the structure with compound **3** with Asp32

Figure 5

Superposition of temperature factor plots of the two molecules of renin in the asymmetric unit of the cubic crystal form in the complex with inhibitor **10** (resolution 2.2 Å). The blue and the red curves correspond to the closed and open forms, respectively. The gap in the region 160 corresponds to a loop which is known to be undefined in all structures of renin described up to now.

Figure 6

Structures of nonpeptide inhibitors complexed with human renin. (a) Superposition of the inhibitor **10** (purple) and CGP 38'560 (**1**, green) in the active site of renin.

(b) Superposition of inhibitors **3** and CGP 38'560 (**1**), detail in the catalytic site. **1** is green, inhibitor **3** is orange, and the two catalytic aspartic acid residues are purple. Arrows point out the relative shift of the P1 nitrogen and hydroxyl oxygen atoms of **3** as compared with **1**. (c) The newly discovered S3^{sp} subsite accommodating the corresponding P3^{sp} residues of three different types of inhibitors superimposed. The active site is rotated by about 90° following the horizontal axis compared to (a,b). The view extends from the catalytic site to the P3^{sp} subpocket. The sidechain of Ser219 was removed from the model before surface calculation. The color codes of the inhibitors are the following: **3** orange, **6** blue, **8** purple. Renin residues are labeled. (d) Superposition of CGP 38'560 (**1**, green) and inhibitor **10** (enzyme shown only) complexes. In the absence of a P2–P3 peptide bond, the His287 sidechain, which forms a water-mediated hydrogen bond with the P3 carbonyl in the peptidic complex, is shifted towards Tyr220 in the presence of **10**. Renin in its complex with **1** is light green, and in the complex with inhibitor **10** (enzyme shown only) in light purple. The figure was prepared using the program GRASP [52].

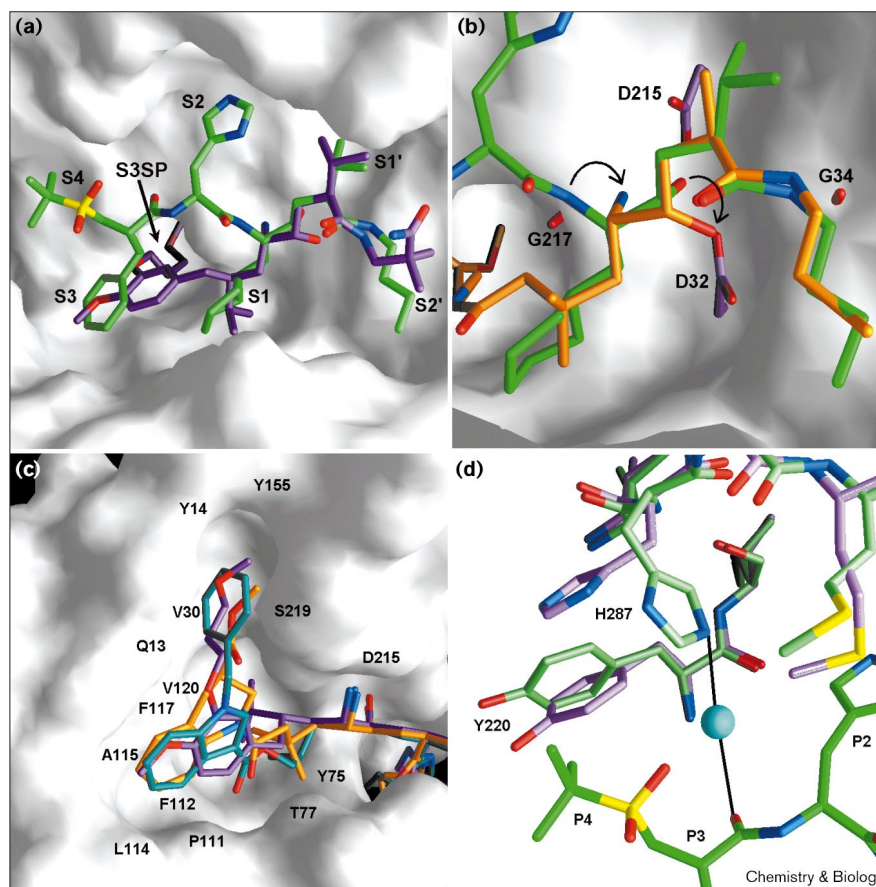


(Figure 7, Table 3). In order to form optimal hydrogen-bond interactions, the NH₂ group is shifted towards the carboxylates of the catalytic residues, and as a consequence the mimetic hydroxyl group is positioned closer to Asp32 than Asp215. In addition, the χ_2 angle of the Asp215 sidechain is shifted by up to 48° as compared with the structure with the peptide inhibitor **1**, moving the Asp215 carboxylate further away from the inhibitor hydroxyl group. Figure 6b illustrates this shift and the formation of a nonsymmetrical hydrogen-bond network of the OH group to both aspartate residues for inhibitor **3** (see also Table 3). The altered hydrogen-bond pattern for nonpeptide compared with peptide-like inhibitors may originate from the electrostatic interaction between the positively charged amino group and the carboxylates of the catalytic residues. Ligand-inducible flexibility of the protein could also facilitate this rearrangement, as could the strong hydrophobic interactions of the inhibitors within the S3/S1 binding pocket. As an exception, the NH₂ group of **9** does not form a hydrogen bond to either of the catalytic aspartates: this can be explained by the shorter all-carbon skeleton of this inhibitor and the shorter distance between the NH₂-bearing carbon and the phenyl group of the P3 moiety. This suggests that the strong

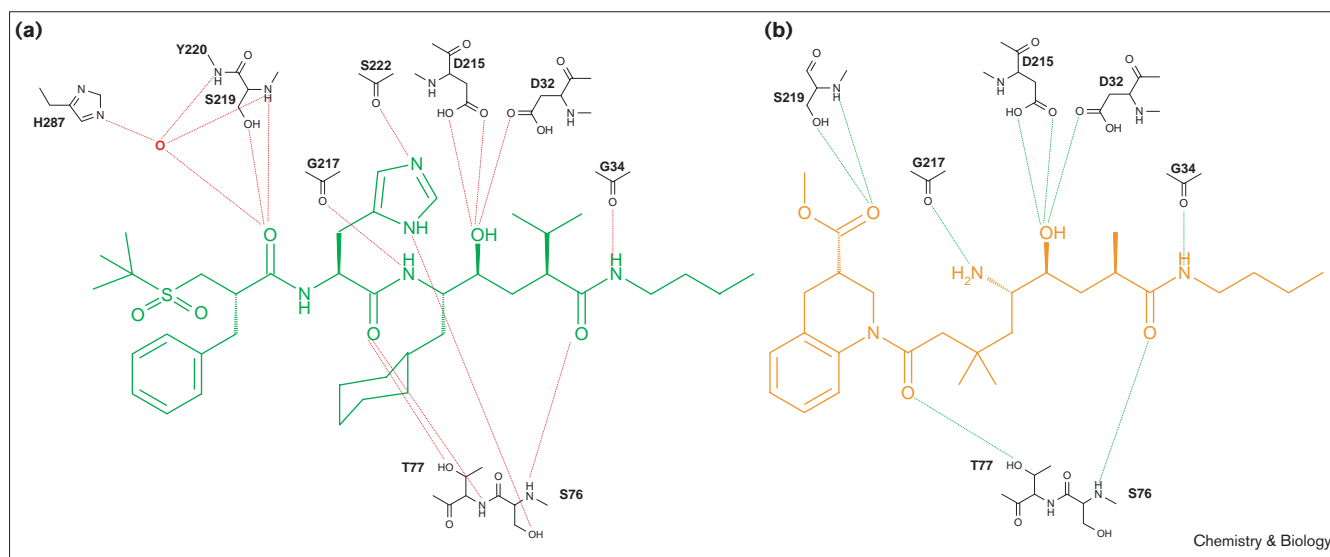
hydrophobic interactions to the S1 and S3 pockets, as well as to the nonsubstrate binding site (see below) play a dominant role with respect to the relative orientation of the inhibitor along the cleft, in contrast to any potential electrostatic effects induced by the inhibitor amine. In contrast, the hydrogen-bonding pattern for compound **10** is again similar to that of compound **3** because of a different P1', P2' moiety.

Table 4

Interactions of the inhibitors in the active site of human renin (residues in renin forming the binding pockets).

S3 ^{sp}	S3	S1	S1'	S2'
Gln13	Thr12	Val30	Ser76	Gly34
Tyr14	Gln13	Asp32	Leu213	Ser35
Val30	Pro111	Tyr75	Asp215	Leu73
Val120	Phe112	Thr77	Ile291	Arg74
Tyr155	Leu114	Phe112	Pro292	Tyr75
Gly217	Ala115	Phe117	Thr295	Gln128
Ala218	Phe117	Val120	Thr298	Ile130
Ser219	Ser219	Asp215	Ala300	
Ala303			Gly217	

Figure 7

Hydrogen-bonding networks of renin bound to inhibitors (a) CGP 38'560 (**1**) and (b) **3**.

Interactions in the specificity pockets

Like the peptide-based CGP 38'560 (**1**), compounds **3–9** are substituted by a *n*-butyl residue at the P2' carboxy-terminal end. This alkyl chain interacts with hydrophobic residues of the corresponding S2' pocket (Table 4). The S1' pocket is partially filled by either a methyl or an isopropyl group similar to the P1' isopropyl in previously published structures [18,20,21]. In all inhibitor structures the hydrophobic P1 residue occupies the S1 pocket. Inhibitors bearing a more bulky P1 isopropyl residue (e.g., compounds **8** and **9**) penetrate more deeply into the S1 pocket. The P1 moiety of the inhibitors together with the adjacent phenyl spacer as in compound **9** constitutes a large hydrophobic entity that is smoothly accommodated by the complementary hydrophobic S1/S3 'superpocket' of the enzyme. The S3 pocket also has a strong preference for hydrophobic aromatic residues as seen for peptide-like inhibitors, although this subsite may also accommodate bulky lipophilic groups [35]. Accordingly, the P3 aryl group of the nonpeptide inhibitors **3, 6–8** is found at roughly the same position within the S3 pocket as the P3 phenyl sidechain of CGP 38'560 (**1**), and as observed in the complex of polyhydroxymonoamide inhibitors to human renin [18,20,21]. The orientation of the P3 moiety in the nonpeptide inhibitors is markedly altered compared with peptide inhibitors, that is the aryl portion is rotated about a horizontal axis by $\sim 30\text{--}40^\circ$ towards Phe117 as compared with the P3 phenyl of inhibitor **1** (Figure 6c). In this orientation the aromatic system fits better to the hydrophobic surface of the contiguous S3–S1 pocket. The X-ray structures of complexes with inhibitors **9** and **10** reveal that the polar methoxy group sits in the S3-binding site, which was expected to bind only bulky hydrophobic

residues. The position of the methyl oxygen atom is roughly within the plane of the P3 aryl of the other inhibitors including **1**, whereas the methyl is pointing towards Leu114, Ala115 and Phe117. The phenyl ring of inhibitors **9** and **10** therefore functions as a hydrophobic spacer connecting the P3-methoxy residue to the P1 isopropyl moiety forms hydrophobic contacts with the sidechains of residues Phe117 and Pro111 at about 4 Å (Table 4). In contrast to **9** and **10**, all other inhibitors (**3–8**) have a polar amide spacer linking the hydrophobic P3 and P1 residues. The carbonyl group of these functionalised spacers forms hydrogen bonds with the sidechain of Thr77 of the flap region. This additional hydrogen-bond interaction may compensate for the weaker van der Waals interactions of inhibitors **3, 6** and **7**, for which a non-optimal fit of the hydrophobic moieties in P1 is observed.

Interactions in the subsite S3^{sp}

The most surprising finding was the binding of the novel nonpeptide inhibitors to a very distinct sub-pocket that has not been exploited previously as an inhibitor-binding site (Figure 6a,c). The crystal structures presented here show that the structurally different substituents of the P3 heterocycle (compare with compounds **3, 4** and **6**) or the P3 spacer phenyl (compare with compounds **7–10**) of the inhibitors all point from the S3 pocket into the same non-substrate cavity. We named this cavity S3 sub-pocket (S3^{sp}). S3^{sp} is oriented perpendicular to the axis of the enzyme cleft and 'points' towards the core of the protein. This channel is about 9 Å deep, corresponding to the length of a six-carbon aliphatic chain. This pocket has also been noted by Tong *et al.* [20]. Substrates or peptide inhibitors do not bind to this sub-pocket as revealed by

the structure of human renin in complex with inhibitor **1**, for example. Instead, water molecules have been located in S3^{sp} [18,20]).

Aromatic and aliphatic amino acid sidechains form the surface of the S3^{sp} sub-pocket. Purely hydrophobic substituents attached to the inhibitor P3 moiety such as the benzyl group of inhibitor **6** can therefore be accommodated in S3^{sp} (Figure 6c). This is in contrast to the proposal of Tong *et al.* [20] who described this pocket as being more polar than the S3-binding site. For inhibitors **7–10**, in addition to hydrophobic contacts, a hydrogen-bond interaction is observed between the distal oxygen of the inhibitor's ether sidechain and the amide nitrogen of Tyr14 (Table 3). The ether oxygen occupies the same position as the oxygen atom of the water molecule in the complex of human renin and CGP 38'560 (**1**; water molecule 370 in PDB entry 1rne). Our structure–activity studies [36–38] have shown that this hydrogen-bond interaction via the terminal ether group contributes only moderately to the *in vitro* binding of such inhibitors. This oxygen atom can be replaced by a hydrophobic –CH₂– group leading to *in vitro* equipotent inhibitors within the different series, possibly due to reduced desolvation energy as compared to the ether analogues. Interestingly, no major conformational changes of the amino acid sidechains flanking the S3^{sp} channel, nor its overall size, were observed between the apo-enzyme structure and the different enzyme–inhibitor complexes.

The carboxylic ester residue at the P3 heterocycle of inhibitor **3** complexed to the enzyme was oriented perpendicular to the axis of the binding cleft, with the terminal–CH₃ directed towards the open S3^{sp} pocket. The ester carbonyl of **3** forms hydrogen bonds with both the backbone amide nitrogen and the O_γ atom of Ser219 (Table 3). The orientation and hydrogen-bond pattern of the enzyme-bound inhibitor through its methyl carboxylate, as discovered by the X-ray analysis, was not anticipated by the initial molecular modelling studies that led to the design of the topological inhibitor **3**. Subsequently, *in vivo* highly potent analogues such as compounds **4** and **5** resulted from replacing the P3^{sp} ester group of **3** by residues that would penetrate more deeply into the S3^{sp} site and that are also more stable towards potential metabolic degradation [29]. Similarly, the proximal P3^{sp} ether oxygen of inhibitors **7–9** is found in a remote position to the entrance of the S3^{sp} subsite and hence are not within binding distance of Ser219 in the enzyme-bound crystal structures as was suggested from modelling [35]. However, in the crystal structure with inhibitor **10**, a water molecule is observed at the entrance of the S3^{sp} pocket, which forms bridging hydrogen bonds with the proximal ether oxygen of the inhibitor P3^{sp} side chain (3 Å) and the hydroxyl group of Ser219 (2.8 Å). The P3 methoxy ether oxygen atom in inhibitor **10** is involved in a hydrogen-bond

network through a water molecule with the hydroxyl group of Thr12 and other water molecules in the P3 pocket.

The topological inhibitors of the new series lack the P2–P4 peptide backbone, the S2 and the S4 pockets are unoccupied and consequently the corresponding extensive hydrogen-bonding network observed in the peptide mimicking, type-I inhibitors [25] is missing (Figure 7). In general, the protein structure in this region of the active site is unchanged in both peptide and nonpeptide inhibitor complexes. There is, however, one exception: the sidechain of His287 has a different orientation in the structures with peptide inhibitors of renin (e.g. CGP 38'560, **1**). Here, the sidechain of His287 forms a water-mediated hydrogen bond with the amide nitrogen atoms of both residues 219 and 220 and the carbonyl P3 of the inhibitor. In contrast, the His287 imidazole ring in the structures containing nonpeptidic inhibitors is rotated about its χ_1 angle by 150° thus forming a hydrophobic contact with Tyr220 (Figure 6d). The same observation was made by Tong *et al.* [20] in the analysis of their polyhydroxymonoamide complexes where His287 was found to be in the same conformation as in the structures of renin with nonpeptidic inhibitors presented here. The lack of the P2–P4 portion of the new inhibitors is partly compensated for by the increased hydrophobic van der Waals contacts within the contiguous S1 and S3 pockets and their large hydrophobic surface, as seen in all crystal complexes of the novel inhibitors, and as reported by others [33,34]. For example, inhibitors **3–5** have affinities to human renin that are more than 50 times stronger than compound **2** (Table 1). We have predicted that mimicking the conserved P3–P2 carbonyl interaction of type-I inhibitors to Ser219 of renin would be important for the proper positioning of the new topological inhibitors within the extended substrate-binding cleft [35]. Also, we assumed that penetration of the P3^{sp} sidechain into the distinct S3^{sp} channel, being flanked at its entrance by Ser219 and oriented perpendicular to the axis of the enzyme cavity, would help to tightly anchor the inhibitor molecule in a favourable position along the cleft relative to the catalytic aspartates, probably before closing of the flap domain upon the ligand. Indeed, the additional hydrophobic and/or hydrogen-bonding interactions to the S3^{sp} sub-pocket or to the Ser219 sidechain hydroxyl group (as in the case of **3**, **10**) are essential for the strong *in vitro* affinity of such inhibitors with IC₅₀ values in the low nanomolar range. The extrusion of several water molecules from the mixed polar–hydrophobic S3^{sp} pocket of the apo-enzyme upon inhibitor binding is obviously entropically/enthalpically favoured, even if the inhibitor bears a highly hydrophobic P3^{sp} residue. In addition, the fact that the number of bound water molecules varies depending on the structure of the complexed type-I inhibitor [18,20] also indicates less tightly bound water molecules within the cavity, in agreement with its partly hydrophobic character.

Protein crystallography has been an integral part of our drug discovery program directed towards the design of a new generation of orally active renin inhibitors. The availability of the three-dimensional structures of several novel nonpeptide inhibitors of different compound series in complex with human renin has provided important and unexpected insight into the binding interactions of such inhibitors, and was thus the basis for a more efficient optimisation of the initial potent lead structures. First, all the inhibitors examined were indeed shown to have a large van der Waals surface interaction with the hydrophobic contiguous S3–S1 binding pocket. These results provided direct experimental evidence for the validity of our original design concept based on a computer modelling hypothesis of tethering an extended hydrophobic (P3–P1)-moiety to a classical transition-state mimetic [30], as has also been demonstrated by others (the discovery of novel potent 3,4,5-trisubstituted piperidines and their X-ray structures in complex with renin have been disclosed during the preparation of this manuscript [39]). Second, the discovery of a distinct channel of human renin that is accessible from the P3 and is an important nonsubstrate binding cavity first for inhibitors **3** and **6** triggered our subsequent medicinal chemistry efforts to focus on the structural optimisation of the inhibitor P3^{sp} sidechain to improve the overall inhibitor profile. Third, on the basis of these findings, new synthetically attractive P3^{sp}–P3 pharmacophores (compounds **7,8**) have rapidly evolved from the iterative design approach [37,38].

Our current understanding of the observed remarkably high enzyme specificity of the reported novel inhibitors for renin versus related aspartic proteases such as pepsin (Table 1), cathepsin D and E [37,38] can be rationalised on the molecular level because only renin possesses the subsite S3^{sp}. More difficult is explaining the significant specificity of the compounds for human renin over renin from some other mammalian species (data not shown). Comparative protein modelling of dog, rabbit or cat renin could help to explain the observed specificity for primate renin as compared to renin of other mammals. The discovery that a water-filled, nonsubstrate pocket that is accessible from the enzyme substrate-binding cleft can serve as an additional or alternative binding site for highly potent topological inhibitors may have general implications for the future design of novel type-III inhibitors of related aspartic acid proteases or proteases of other families of therapeutic interest.

Significance

Inhibiting renin to treat hypertension appears to be attractive because of the high specificity and unique role of this enzyme in the renin–angiotensin cascade. Renin is known to exclusively catalyse the cleavage reaction that produces angiotensin I from angiotensinogen. Renin inhibitors are therefore expected to avoid the adverse

side effects sometimes observed with compounds that interfere with other proteins of this cascade, (e.g. angiotensin-converting enzyme, ACE). In clinical trials several type I (peptide-like) renin inhibitors reduced high blood pressure in patients with similar pharmacological efficacy as compared to ACE inhibitors [22]. All potent renin inhibitors investigated to date, however, show insufficient oral bioavailability or short duration of action requiring high oral dosing, and therefore are unlikely to be useful as therapeutic agents.

The concerted effort using molecular modelling techniques, crystallographic structure elucidation and biological assays has led to the design of novel, highly potent and selective nonpeptide inhibitors of human renin. These small-molecule inhibitors have favourable physicochemical properties, such as remarkably good water solubility and low lipophilicity as compared to type-I inhibitors, and are resistant to rapid biodegradation by peptidases in the intestinal tract, blood circulation and liver. Several of these compounds including **4**, **5** [29] and **7–10** [36–38] showed good oral absorption in marmoset monkeys (see the Materials and methods section). Inhibitor **10**, which has sub-nanomolar binding affinity and is highly specific for human renin has pronounced *in vivo* activity in primates after oral administration. It has been selected as a candidate for clinical trials and is presently under clinical investigation by Speedel Pharma AG, Basel.

Materials and methods

Renin and inhibitors

Prorenin was cloned and expressed in Chinese hamster ovary cells, purified by affinity chromatography using a monoclonal antibody and activated using immobilised trypsin as previously described [40] to obtain recombinant glycosylated human renin. Synthesis of inhibitors **7–10** has been reported in preliminary communications [36–38]. The synthesis of the other nonpeptide inhibitors mentioned here will be disclosed in due course. *In vitro* potencies of compounds against purified human recombinant renin were determined as described in [26].

Crystallography

Crystals of recombinant glycosylated human renin were grown as described in Lim *et al.* [41]. The crystals belong to the space group P2₁3 with a = b = c = ~143.0 Å. There are two molecules of renin per asymmetric unit. These crystals were used for inhibitor soaking experiments. Inhibitor-enzyme cocrystallisation experiments (inhibitor **7**) provided tetragonal crystals belonging to space group P4₁2₁2 with a = b = 98.4 and c = 95.6 Å [18]. For inhibitor **10**, recombinant glycosylated human renin was cocrystallised with the inhibitor in 0.6 M ammonium acetate, 12% (w/v) PEG 4000 and 0.1 M sodium citrate buffer pH 3.0. The crystals obtained were cubic and belong to space group P2₁3 with two molecules in the asymmetric unit and a = b = c = 141.6 Å. For soaking experiments (inhibitors **3**, **6**, **8** and **9**), a crystal of renin was soaked into a glass capillary with a small amount of the reservoir solution and a small amount of the inhibitor was suspended into the solvent close to the crystal. After 30 min to 1 h the solution was removed from the crystals for data collection.

X-ray diffraction data were collected using a FAST area detector (Delft Instruments, The Netherlands) positioned on a FR571 rotating anode X-ray generator (Delft Instruments) operated at 40 kV and 70 mA pro-

ducing CuK α graphite monochromated radiation and having an apparent focal spot of 0.3 \times 0.3 mm². The crystal-to-detector distance was 80 mm for the cubic crystals and 60 mm for the tetragonal crystal. The detector was positioned at a swing-out angle of 15°. Frames of 0.1° were collected; the exposure time was 2 min per frame. The frames were processed by the program MADNES [42] the measured data were processed and merged using the CCP4 program suite [43].

X-ray diffraction data for the inhibitor 10–renin complex crystals were collected at 100 K using a MAR image plate mounted on a FR 591 rotating anode generator (Enraf-Nonius) operating at 4.1 kW and producing graphite monochromated CuK α radiation. 81 frames were collected (exposure: 3 passes of 10 min each, crystal rotation: 0.5° per frame). The data were processed and scaled using the MARXDS and the MARSCALE software programs [44]. Data collection and statistics are summarised in Table 2.

The structures were determined by applying difference Fourier methods, using the models previously obtained for both tetragonal and cubic crystals [18]. Although the cubic crystal form contains two molecules in the asymmetric unit, they were refined separately and no molecular averaging was applied because it has been observed previously that the two molecules are in different conformations, an 'open' and 'closed' form. The inhibitors were positioned in the active site by superposition on F_{obs}–F_{calc} maps. The structures were then refined using programs TNT [45] or XPLOR [46] (Table 2). Manual rebuilding of the models was performed with the program O [47]. For the complex with 10, all reflections were used and a solvent correction was applied. A free R_{factor} of 0.266 was obtained for this complex.

In vivo studies

Oral administration of the novel inhibitors to conscious, unrestrained (telemetered) and Na⁺-depleted marmosets [48] resulted in a pronounced long lasting (up to 24 h) and dose dependent (1–10 mg/kg p.o.) reduction of mean arterial pressure (MAP) paralleled by complete inhibition of plasma renin activity *in vivo*. Δ MAP_{max} = 25–30 mmHg was observed during the first 4 h (3 mg/kg dose) for compound 10.

Acknowledgements

We thank J. Priestle for helpful discussions. Furthermore, F. Lugin, N. Hasler, C. Glaser-Rochat, U. Diessenbacher, H.-P. Baum and Ch. Schnell are acknowledged for their skillful technical assistance.

References

- Reid, I.A., Morris, R.J. & Ganong, W.F. (1978). The renin–angiotensin system. *Ann. Rev. Physiol.* **40**, 377–410.
- Skeggs, L.T., Doven, F.E., Levins, M., Lentz, K. & Kahn, J.R. (1980). The biochemistry of the renin-angiotensin system. In *The Renin–Angiotensin System*. (Johnson, J.A. & Anderson, R.R., eds), pp. 1–27, Plenum Press, New-York.
- Hofbauer, K.G. & Wood, J.M. (1985). Renin inhibitors as possible antihypertensive agents. *Klin. Wochenschr.* **66**, 906–913.
- Sweet, C.S. & Blaine, E.H. (1984). Angiotensin converting enzyme inhibitors. In *Handbook of Hypertension*. (Zanchetti, A. & Tarazzi, R.C., eds), pp. 343–363, Elsevier, Amsterdam, The Netherlands.
- Johnston, C.I. (1984). Angiotensin converting enzyme inhibitors. In *Handbook of Hypertension*. (Zanchetti, A. & Tarazzi, R.C., eds), pp. 272–311, Elsevier, Amsterdam, The Netherlands.
- Zanchetti, A. & Tarazzi, R.C. (1982). Symposium on angiotensin-converting enzyme, a developing therapeutic concept. *Am. J. Cardiol.* **49**, 1381–1579.
- Hofbauer, K.G., Hulthén, L.U. & Bühler, F.R. (1983). Antagonists and inhibitors of the renin-angiotensin system for the treatment of hypertension. In *Hypertension, Physiopathology and Treatment*. (Genest, J., Kuchel, O., Hamet, P. & Cantin, M., eds) pp. 1225–1238, McGraw-Hill, New-York.
- Brunner, N.R., Nussberger, J. & Waeber, B. (1985). Effects of angiotensin converting enzyme inhibition: a clinical point of view. *J. Cardiovasc. Pharmacol.* **7**(Suppl 4), 73–81.
- Waeber, B., Nussberger, J. & Brunner, H.R. (1995). Angiotensin-converting enzyme inhibitors in hypertension. In *Hypertension: Pathophysiology, Diagnosis and Management*, 2nd edition. (Laragh, J.H. & Brenner, B.M., eds) pp. 2861–2876, Raven Press, New York.
- Ondetti, M.A. & Cushman, D.W. (1982). Enzymes of the renin–angiotensin system and their inhibitors. *Ann. Rev. Biochem.* **51**, 283–308.
- Antonaccio, M.J. (1982). Inhibitors of the renin–angiotensin system as new antihypertensive agents. *Clin. Exp. Hypertens. A* **4**, 27–46.
- Hofbauer, K.G. & Wood, J.M. (1986). The renin–angiotensin system, inhibitors and antagonists. In *Handbook of Hypertension*, volume 8 (Zanchetti, A., & Tarazzi, R.C., eds) pp. 466–488, Elsevier, Amsterdam, The Netherlands.
- Nelson, E.B., Harm, S.C., Goldberg, M., Shahinfar, S., Goldbeg, A. & Sweet, C.S. (1995). Clinical profile of the first angiotensin II (AT-1 specific) receptor antagonists. In *Hypertension: Pathophysiology, Diagnosis and Management*, 2nd edition. (Laragh, J.H. & Brenner, B.M., eds) pp. 2895–2916, Raven Press, New York.
- Chen, K.C.S. & Tang, J. (1972). Amino acid sequence around the epoxide-reactive residues in pepsin. *J. Biol. Chem.* **247**, 2566–2574.
- Hartsuck, J.A. & Tang, J. (1972). The carboxylate ion in the active centre of pepsin. *J. Biol. Chem.* **247**, 2575–2580.
- Grütter, M.G. & Rahuel, J. (1995). Human renin: biochemistry, crystal structure, and opportunities for development of specific inhibitors. In *Hypertension: Pathophysiology, Diagnosis and Management*, 2nd edition. (Laragh, J.H. & Brenner, B.M., eds) pp. 1607–1619, Raven Press, New York.
- Sielecki, A.R., *et al.*, & James, M.N.G. (1989). Structure of recombinant human renin, a target for cardiovascular-active drugs, at 2.5 Å resolution. *Science* **243**, 1346–1351.
- Rahuel, J., Priestle, J.P. & Grütter, M.G. (1991). The crystal structures of recombinant glycosylated human renin alone and in complex with a transition-state analog inhibitor. *J. Struct. Biol.* **107**, 227–236.
- Dhanaraj, V., *et al.*, & Hoover, D.J. (1992). X-ray analyses of peptide–inhibitor complexes define the structural basis of specificity for human and mouse renins. *Nature* **357**, 466–472.
- Tong, L., *et al.*, & Jung, G. (1995). High resolution crystal structures of recombinant human renin in complex with polyhydroxymonoamide inhibitors. *J. Mol. Biol.* **250**, 211–222.
- Tong, L., Pav, S., Lamarre, D., Simoneau, B., Lavallée, P. & Jung, G. (1995). Crystallographic studies on the binding modes of P2–P3 butanediamide renin inhibitors. *J. Biol. Chem.* **270**, 29520–29524.
- Wood, J., Cumin, F. & Maibaum, J. (1994). Pharmacology of renin inhibitors and their application to the treatment of hypertension. In *Pharmac. Ther.* (Heagerty, A.M., ed.), pp 325–344, Elsevier Science Ltd, UK.
- Szelke, M., *et al.*, & Lever, A.F. (1982). Potent new inhibitors of human renin. *Nature* **299**, 555–557.
- Boger, J., *et al.*, & Bopari, A.S. (1983). Novel renin inhibitors containing the amino acid statin. *Nature* **303**, 81–84.
- Ripka, A.S. & Rich, D.H. (1998). Peptidomimetic design. *Curr. Opin. Chem. Biol.* **4**, 439–452.
- Bühlmayer, P., *et al.*, & Wood, J.M. (1988). Synthesis and biological activity of some transition-state inhibitors of human renin. *J. Med. Chem.* **31**, 1839–1846.
- Schechter, I. & Berger, A. (1967). On the size of the active site of proteases. I. Papain. *Biochem. Biophys. Res. Commun.* **27**, 157–162.
- Wood, J.M., *et al.*, & Kay, J. (1989). CGP 38560: Orally active, low molecular weight renin inhibitor with high potency and specificity. *J. Cardiovasc. Pharmacol.* **14**, 221–226.
- Maibaum, J., *et al.*, & Wood, J.M. (1996). Design and synthesis of novel potent, nonpeptide and orally active renin inhibitors. In *Medicinal Chemistry: Today and Tomorrow*. (Gujral, P.D., ed.), pp 155–162. Blackwell Science Ltd., Oxford.
- Rasetti, V., *et al.*, & Wood, J.M. (1996). Bioactive hydroxyethylene dipeptide isosteres with hydrophobic (P3–P1)-moieties. A novel strategy towards small nonpeptide renin inhibitors. *Bioorg. Med. Chem. Lett.* **6**, 1589–1594.
- Sibanda, B.L., *et al.*, & Chirgwin, J.M. (1984). Computer graphics modelling of human renin. Specificity, catalytic activity and intron–exon junctions. *FEBS Lett.* **174**, 102–111.
- Cohen, N.C. (1989). Molecular mimics and drug design. *Trends in Medicinal Chemistry* **88** (van der Goot, H., Domány, L., Pallos, L. & Timmerman, H., eds), pp 13–28, Elsevier, Amsterdam.
- Plummer, M., *et al.*, & Rapundalo, S.T. (1995). Design and synthesis of renin inhibitors. Incorporation of transition-state isostere sidechains that span from the S1 to the S3 binding pockets and examination of P3-modified renin inhibitors. *J. Med. Chem.* **38**, 2893–2905.
- Leffer, B.A., *et al.*, & Sneddon, S.F. (1995). Rational design, synthesis and X-ray structure of renin inhibitors with extended P1 sidechains.

- Bioorg. Med. Chem. Lett.* **5**, 2623-2626.
35. Göschke, R., Cohen, N.C., Wood, J.M. & Maibaum, J. (1997). Design and synthesis of novel 2,7-dialkyl substituted 5(S)-4(S)-hydroxy-8-phenyl-octanecarboxamides as *in vitro* potent peptidomimetic inhibitors of human renin. *Bioorg. Med. Chem. Lett.* **7**, 2735-2740.
 36. Göschke, R., *et al.*, & Maibaum, J. (1998). Novel 2,7-dialkyl substituted 5(S)-amino-4(S)-hydroxy-8-phenyl-octanecarboxamide transition state peptidomimetics are potent and orally active inhibitors of human renin. *XVth EFMC Int. Symp. Med. Chem, Edinburgh (UK)*, 6–10 Sept 1998; Abstract Book, p. 229.
 37. Maibaum, J., *et al.*, & Wood, J.M (1998). Design and synthesis of novel, fully non-peptide transition state mimetic renin inhibitors bearing an O-alkyl substituted salicylamide (P3^{SP}-P3)-moiety with high oral *in vivo* potency. *XVth EFMC Int. Symp. Med. Chem, Edinburgh (UK)*, 6-10 Sept 1998; Abstract Book, p. 231.
 38. Maibaum, J., *et al.*, & Wood, J.M. (1998). Structural modification of the P2' position of 2,7-dialkyl substituted 5(S)-amino-4(S)-hydroxy-8-phenyl-octanecarboxamides: discovery of a potent non-peptide human renin inhibitor active after once daily dosing in marmosets. *XVth EFMC Int. Symp. Med. Chem, Edinburgh (UK)*, 6–10 Sept 1998; Abstract Book, p. 230.
 39. Oefner, C., *et al.*, & Wostl, W. (1999). Renin inhibition by substituted piperidines: a novel paradigm for the inhibition of monomeric aspartic proteinases? *Chem. Biol.* **6**, 127-131.
 40. Asselbergs, F.A.M., Rahuel, J., Cumin, F. & Leist C. (1994). Scaled-up production of recombinant human renin in CHO cells for enzymatic and X-ray structure analysis. *J. Biotechnol.* **32**, 191-202.
 41. Lim, L.W., Stegeman, R.A., Leimgruber, N.K., Gierse, J.K., & Abdel-Meguid, S.S. (1989). Preliminary crystallographic study of glycosylated recombinant human renin. *J. Mol. Biol.* **210**, 239-240.
 42. Messerschmidt, A. & Pflugrath, J.W. (1987). Crystal orientation and X-ray pattern prediction for area-detector diffractometer systems in macromolecular crystallography. *J. Appl. Crystallogr.* **20**, 306-315.
 43. Collaborative Computational Project, Number 4 (1994). The CCP4 suite, programs for protein crystallography. *Acta Crystallogr. D* **50**, 760-763 .
 44. Kabsch, W. (1988). Evaluation of a single crystal diffraction form a position-sensitive detector. *J. Appl. Crystallogr.* **21**, 916-924.
 45. Tronrud, D.E., Ten Eyck, L.F. & Matthews, B.W. (1987). An efficient general-purpose least-square refinement program for macromolecular structures. *Acta Crystallogr. A* **43**, 489-501.
 46. Brünger, A.T. (1992). *X-PLOR Version 3.1 A system for X-ray Crystallography and NMR*. Yale University Press. New Haven and London, UK.
 47. Jones, A.T., Zou, J.-Y., Cowan, S.W. & Kjeldgaard, M. (1991). Improved methods for building protein models in electron density maps and the location of errors in these models. *Acta Crystallogr. A* **47**, 110-119.
 48. Schnell, C.R. & Wood, J.M. (1993). Measurement of blood pressure and heart rate by telemetry in conscious, unrestrained marmosets. *Am. J. Physiol.* **264**, H1509-1516.
 49. Kraulis, P. (1991). MOLSCRIPT: a program to produce both detailed and schematic plots of protein structures. *J. Appl. Cryst.* **24**, 946-950.
 50. Bacon D.J. & Anderson W.F. (1998). A fast algorithm for rendering space-filling molecule pictures. *J. Mol. Graph.* **6**, 219-220.
 51. Merritt, E.A. & Murphy M.E.P. (1994). Raster3D version2.0 – a program for photorealistic molecular graphics. *Acta Crystallogr. D* **50**, 869-873.
 52. Nichols, A., Sharp K.A. & Honig, B. (1991). Protein folding and association: insights from the interfacial and thermodynamic properties of hydrocarbons. *Proteins* **11**, 281-296.